

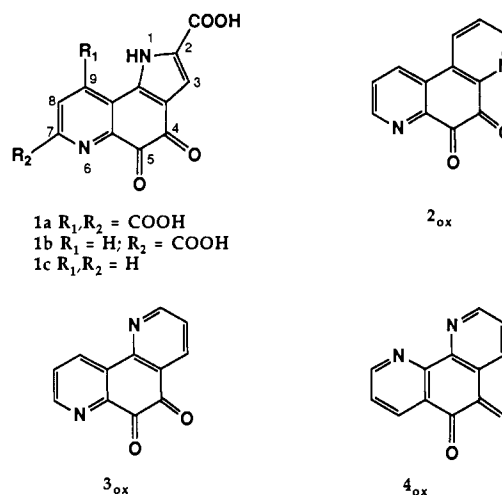
Reaction of Methoxatin and 9-Decarboxymethoxatin with Benzylamine. Dynamics and Products

Evelyn J. Rodriguez and Thomas C. Bruice*

Contribution from the Department of Chemistry, University of California at Santa Barbara, Santa Barbara, California 93106. Received March 13, 1989

Abstract: The pH dependence of kinetics and products in the oxidation of benzylamine by methoxatin (**1a**) and 9-decarboxymethoxatin (**1b**) has been determined as has the pH dependence of the hydration of **1a** and **1b** (25 °C in water, $\mu = 1.0$ with KCl). The hydration equilibria for **1a** and **1b** are quite comparable. Thus, the pK_{app} for hydration of **1a** is 10.51, and for **1b** the value is 10.73. The rates of hydration and dehydration of **1a** and **1b** were determined to be instantaneous on the time scale for the reduction of these quinones by benzylamine. Rates of oxidation of benzylamine free base by **1a** and **1b** are quite similar at constant pH values, between pH 6.5 and 12.3. Thus, the biologically important 9-carboxyl group of methoxatin does not contribute significantly to either its hydration equilibria or its rates of amine oxidation. Oxidation of benzylamine free base (Am_f) by **1a** and **1b** is first and second order in Am_f ($k_A[Am_f][Q] + k_B[Am_f]^2[Q]$; where Q is unhydrated **1a** or **1b**). The apparent second- and third-order rate constants k_A and k_B are pH dependent. The first step in the oxidations is the reversible formation of neutral (CA) and protonated (CAH^+) carbinolamine of Am_f and Q. CA and CAH^+ proceed to products via (i) general-base α -benzylic proton abstraction and elimination to yield diol species (**11a** and **11b**) plus the ammonia imine of benzaldehyde and (ii) H_2O -, H_3O^+ -, or HO^- -catalyzed dehydration providing quinone-benzylamine imine (Im1), which undergoes general-base α -benzylic proton abstraction and elimination to provide the aminophenol imine of benzaldehyde (Im2). Hydrolysis of Im2 provides aminophenols (**10a** and **10b**) plus benzaldehyde. From its pH dependence, the k_A term relates to H_2O -catalyzed decomposition of CAH^+ and both H_2O - and HO^- -catalyzed decomposition of CA. The species H_2O and HO^- act as general-base catalysts to abstract the α -benzylic proton of the carbinolamine species to generate directly the diol species **11a** and **11b** plus the ammonia imine of benzaldehyde (Scheme II). The kinetic deuterium isotope effects associated with H_2O and HO^- general-base catalysts ($k_A^H/k_A^D = 14.3$ at pH 8.8 and 3.6 at pH 11.7) were obtained from parallel experiments employing $PhCH_2NH_2$ and $PhCD_2NH_2$. The k_B term provides the predominant reaction paths in the oxidation of benzylamine. In going from low to high pH, diol formation increases at the expense of aminophenol formation (Table I) and the k_B term changes from dependence upon $[H_3O^+]^2$, to dependence on $[H_3O^+]$, to an independence upon $[H_3O^+]$, and finally to dependence upon $[HO^-]$. The rate constants for these four regions of pH are, respectively, k_d , k_e , k_f , and k_g (Chart II). The mechanism associated with k_d (Scheme VIc) involves H_3O^+ -catalyzed dehydration of CA to provide Im1 followed by benzylamine general-base abstraction of the α -benzylic proton of $Im1H^+$ to yield Im2. Hydrolysis of Im2 provides aminophenols (**10a** and **10b**) plus benzaldehyde. The k_e term expresses two reaction paths. The first involves benzylamine general-base-catalyzed α -proton removal from CAH^+ , yielding diol (Scheme Vc), and the second H_3O^+ -catalyzed dehydration of CA to provide Im1, followed by benzylamine general-base abstraction of the α -benzylic proton from Im1 to form Im2, which goes on to provide **10a** and **10b** as before (Scheme VII). Associated with the term k_f is the benzylamine general-base-catalyzed formation of diol from CA and the spontaneous or H_2O -catalyzed dehydration of CA to provide Im1, followed by abstraction of the α -benzylic proton from Im1 by benzylamine to form Im2, which upon hydrolysis provides **10a** and **10b** (Scheme VII). The term k_g involves HO^- -catalyzed dehydration of CA followed by removal of the α -benzylic proton from Im1 by benzylamine and subsequent hydrolysis of Im2 to provide aminophenol as product (Scheme VII). The kinetic deuterium isotope effect (k_B^H/k_B^D) of 5.7 was obtained at pH 8.8 and 11.7. These isotope effects pertain to the second term of k_e as well as k_f and k_g . In separate experiments, the kinetics for the formation of diol **11a** from aminophenol **10a** on oxidation of the latter by methoxatin was studied. The rate constants associated with this process are such that the yields of aminophenol and diol, produced on reaction of benzylamine with quinone, are not influenced by formation of diol by reaction of aminophenol product with remaining quinone above pH 7. Below pH 7 reaction of quinone with aminophenol is more facile than is benzylamine oxidation such that the latter determines the product.

Since the elucidation of its structure in 1979,¹ methoxatin (**1a**), also referred to as PQQ or pyrroloquinoline-quinone) has been reported to be the cofactor in numerous oxidoreductases, appearing in organisms as diverse as bacteria and man.² Enzymes for which methoxatin has been reported to serve as coenzyme are involved in the oxidation of aldoses,³ primary alcohols,⁴ and primary amines.⁵ Mechanisms for the oxidation of alcohols⁶ and amines^{2,7}



by quinoproteins have been proposed. The structural features of the cofactor that are important for enzymatic activity may be

(1) (a) Salisbury, S. A.; Forrest, J. S.; Cruse, W. B. T.; Kennard, O. *Nature* **1979**, *280*, 843. (b) Westerling, J.; Frank, J.; Duine, J. A. *Biochem. Biophys. Res. Commun.* **1979**, *87*, 719.

(2) For recent reviews, see: (a) Hartmann, C.; Klinman, J. P. *Biofactors* **1988**, *1*, 41. (b) Duine, J. A.; Frank, J.; Jongejan, J. A. *Adv. Enzymol.* **1987**, *59*, 170.

(3) Duine, J. A.; Frank, J.; van Zeeland, J. K. *FEBS Lett.* **1979**, *108*, 443.

(4) (a) Anthony, C. In *The Biochemistry of Methylotrophs*; Academic: New York, 1982. (b) Duine, J. A.; Frank, J. *J. Gen. Microbiol.* **1981**, *122*, 201. (c) Groen, B.; Frank, J.; Duine, J. A. *Biochem. J.* **1984**, *223*, 921.

(5) (a) McIntire, W. S.; Stults, J. *Biochem. Biophys. Res. Commun.* **1986**, *141*(2), 562. (b) Knowles, P. F.; Yadav, K. D. S. In *Copper Proteins and Copper Enzymes*; Lontie, R., Ed.; CRC Press: Boca Raton, FL, 1984; Vol. II, p 103.

(6) (a) Forrest, H. S.; Salisbury, S. A.; Kilty, C. G. *Biochem. Biophys. Res. Commun.* **1980**, *97*, 248. (b) de Beer, R.; Duine, J. A.; Frank, J.; Westerling, J. *Eur. J. Biochem.* **1983**, *130*, 105. (c) Dijkstra, M.; Frank, J.; Jongejan, J. A.; Duine, J. A. *Eur. J. Biochem.* **1984**, *140*, 369.

(7) Farnum, M.; Palcic, M.; Klinman, J. P. *Biochemistry* **1986**, *25*, 1898.

further purification. 9-Decarboxymethoxatin (**1b**) was available from a previous study.⁹

Instrumentation. Kinetic traces and UV/vis spectra were recorded using a Uvikon 810 spectrophotometer equipped with a thermostated cell holder at 25 ± 0.2 °C (path length 1 cm). The spectrophotometer was housed in an oxygen-free nitrogen atmosphere. A Radiometer Model M26 pH meter and a Fischer pencil-thin gel-filled combination electrode or a Metrohm combination electrode were used for pH measurements. HPLC analysis was performed under the following conditions: the apparatus consisted of an Altex 100 dual stroke pump, an Altex-Beckman Ultrasphere ODS analytical column (5 μ m, 4.6×250 mm), a 10- μ m Ultrapack precolumn, a Rheodyne injector with a 100- μ L loop, an HP 1040A diode-array UV detector, and an HP 3392A integrator. The system was interfaced to an HP 85B computer and operated by HP software designed for UV measurements. The flow rate was 0.6 mL/min.

Kinetic Studies. Solutions were prepared with total concentration of amine ($[Am_t]$) ranging from 0.015 to 0.15 M ($\mu = 1.0$, KCl) and a quinone concentration ($[Q]$) of 3.8×10^{-5} M. Below pH 8, phosphate buffers were used to maintain constant pH, between pH 8 and 10, benzylamine was used as buffer and reactant, and above pH 10, hydroxide ion was employed as a buffer. All reactions were run at 25 ± 0.2 °C in a nitrogen-filled glovebox and followed by monitoring the appearance of product formed by reduction of the quinone, in the case of **1b**, at 294 nm (<pH 10) and 311 nm (>pH 10), and for **1a**, at 300 nm (<pH 10) and 320 nm (>pH 10). Reactions were initiated by adding 10 μ L of a stock solution of **1a** or **1b** (in DMSO) to the thermostated amine solution in a nitrogen-filled glovebox. Deuterium isotope experiments were performed under the same conditions and in parallel with the experiments employing nondeuterated materials.

Buffer dilution experiments were carried out with a $[Am_t]$ of 0.1 M ($[Am_f] = 2.7 \times 10^{-5}$ M to 9.62×10^{-4} M). Total buffer concentration ranged from 0.01 to 0.53 M depending on the pH. No buffer catalysis by phosphate was detected below pH 8.

For product analysis $[Q_t] = 7.6 \times 10^{-5}$ M and $[Am_t] = 0.05$ M. The spent reaction mixture was acidified with dilute HCl to pH 4 and immediately injected in the HPLC using a gas-tight syringe. These solutions were analyzed by monitoring the absorbance at or near the isobestic point of the normalized spectra of the diol and the aminophenol at pH 3 (at 300 nm for **1a** and 293 nm for **1b**). The eluent (50/50/0.03 MeOH/H₂O/85% H₃PO₄, v/v/v; pH 3), was purged for 1 h with argon prior to the analysis and maintained with a head of argon throughout the analysis. Retention times and UV/vis spectra for **1a** and **1b**, quinols **11a** and **11b**, PhCH₂NH₂, and PhCHO were compared to those of authentic samples.

Identification of aminophenol 10a was performed as follows: **1a** (5 mg) was treated with a 20-fold excess of benzylamine in an aqueous solution (5 mL) at pH 8.5 in a nitrogen-filled glovebox. The solution was allowed to stand at room temperature for 24 h and then extracted with ether to remove unreacted benzylamine and PhCHO. The aqueous phase was adjusted to pH > 9 (KOH) and extracted with ether to remove all remaining benzylamine. The aqueous layer was then concentrated, and products were separated by thin-layer chromatography (Whatman reversed-phase KCl8F, 200 μ m, 20×20 cm), using 4/3 MeOH/H₂O (v/v). The aminophenol separated as a yellow band and was eluted with MeOH. Air oxidation of this compound regenerated methoxatin as determined by HPLC and UV/vis analysis. Ammonia evolution upon aerobic reoxidation was confirmed by a modification of the Nessler technique¹⁵ and agreed within 25% of the concentration of **1a** determined from the absorbance of an air-oxidized solution of the aminophenol.

Oxidation of aminophenol 10a by methoxatin (25 °C, $\mu = 1.0$) was initiated by adding 2 μ L of a 1.14×10^{-2} M **1a** stock solution (DMSO) to 1.5 mL of a thermostated buffer containing 20 μ L of a 4.5×10^{-3} M stock solution (MeOH) of **10a**. Aminophenol oxidation was studied from pH 6.03 to 12.02 under an inert atmosphere. pH was maintained by use of phosphate (pH 6.03–7.77), borate (pH 8.95), carbonate (pH 9.72), and hydroxide buffers (pH > 10.8). The reaction was monitored by following the appearance of diol **11a** at 300 or 310 nm. Complete formation of diol from aminophenol was confirmed by HPLC analysis of the reaction mixture.

Results

All experiments have been carried out in water at 25 °C at $\mu = 1.0$ (with KCl) under an atmosphere of O₂-free N₂. The pK_a of benzylamine was determined by spectrophotometric titration (225 nm). Least-squares fitting of the titration curve gave a pK_a of 9.57. In the pH range employed (pH 6.5–12.3) for kinetic

studies the carboxyl groups of methoxatin (**1a**) and 9-decarboxymethoxatin (**1b**) are dissociated and the pyridine nitrogens are not protonated.^{9,11b} Below pH 8, phosphate or imidazole buffers were employed, and above pH 8, benzylamine/benzylamine-H⁺ and HO⁻/H₂O were employed to maintain constant pH. Catalysis of benzylamine oxidation by H₂PO₄⁻/HPO₄²⁻ was not observed. On the other hand, the reaction is subject to imidazole catalysis. The lack of general catalysis by an oxy anion base, but the observation of catalysis by a nitrogen base of like pK_a may be attributed to electrostatic repulsion and attraction, respectively, in the transition state¹⁶ or to a nonproductive interaction of the oxy anion with quinone (vide infra, see Oxidation of Aminophenol). Buffer catalysis, by other than benzylamine substrate, has received only cursory examination.

pH Dependence of the Hydration of Methoxatin (1a). From eq 1a the hydration of *o*-quinones is initiated by HO⁻ addition. The apparent pK_a (i.e., pK_{app}) for **1a** hydration was determined by spectrophotometric titration. A $pK_{app} = 10.51$ was obtained from least-squares analysis of titration curves obtained from the decrease in A_{275} and A_{300} from pH 5.0 to 12.0 (for **1a** $\epsilon_{275} = 16800$ M⁻¹ cm⁻¹, $\epsilon_{330} = 10700$ M⁻¹ cm⁻¹, and for hydrated **1a** $\epsilon_{275} = 12500$ M⁻¹ cm⁻¹, $\epsilon_{330} = 9900$ M⁻¹ cm⁻¹). This value may be compared to 10.73 for the hydration of 9-decarboxymethoxatin (**1b**).¹⁷ From eq 1a, $K_{app} = K_w K_1 (1 + K_2)$ and the absorbance changes (ΔA) with change of pH are provided by eq 3.

$$\Delta A = \frac{a_H}{K_w K_1 (1 + K_2) + a_H} \quad (3)$$

The hydration and dehydration of the quinones was determined to be rapid. Thus, when an aqueous solution of **1b** (3.8×10^{-5} M) was diluted with an equal volume of 0.1 M KOH, changes in A_{275} and A_{300} were found to be too rapid to follow by ordinary spectral observation. When conversion of hydrate to quinone was carried out by addition of an excess of 1 M phosphate buffer (pH 7) to a 0.01 M KOH solution, which was 3.8×10^{-5} M in **1b**, dehydration was found to be complete at the time of mixing.

Benzylamine oxidation by methoxatin (1a) and 9-decarboxymethoxatin (1b) was carried out under the pseudo-first-order condition of total benzylamine concentration ($[Am_t]$, 0.015–0.10 M) \gg total quinone concentration ($[Q_t]$, 3.8×10^{-5} M). Appearance of quinone reduction products was monitored by following the increase in A_{294} (<pH 10) and A_{311} (>pH 10) for **1b** and A_{300} (<pH 10) and A_{320} (>pH 10) for **1a**. The final spectrum of the reaction mixture resembled that of the hydroquinones **11a** or **11b**. (It is not possible to differentiate **11a** or **11b** from the corresponding aminophenols **10a** and **10b** by UV spectra.) Exposure of the spent reaction solutions to air regenerated the spectrum of the starting quinone species.

At the given wavelengths, the changes in absorbance on reaction of **1a** (pH 6 to 11.5), or **1b** (<pH 10), with benzylamine followed the first-order rate law. Above pH 10 the change in absorbance with time for the oxidation of benzylamine by **1b** was biphasic and could be fit by the equations for two consecutive pseudo-first-order reactions. Repetitive spectral scanning showed no accumulation of an intermediate. The second reaction becomes important for only the last 10–15% change in absorbance, and the pseudo-first-order rate constants determined from this portion of the kinetic plot are not used in the analysis of data.

Plots of the pseudo-first-order rate constants (k_{obs}) for oxidation of benzylamine by **1a** or by **1b** vs the concentration of benzylamine free base ($[Am_f]$) exhibit upward curvature. This indicates a greater than first-order dependence on amine concentration. Throughout the pH range studied, plots of $k_{obs}/[Am_f]$ vs $[Am_f]$ were linear with positive intercepts (Figure 1), indicative of a rate law that is both first-order and second-order in amine (eq 4). The

$$\frac{-d[Q_f]}{dt} = (k_A + k_B [Am_f]) [Am_f] [Q_f] \quad (4)$$

(16) Bruice, P. Y. *J. Am. Chem. Soc.* **1984**, *106*, 5959 and references therein.

(17) Rodriguez, E. J.; Bruice, T. C.; Edmondson, D. E. *J. Am. Chem. Soc.* **1987**, *109*, 532.

(15) Mayer, S. W.; Kelly, F. H.; Morton, M. E. *Anal. Chem.* **1955**, *27*, 837.

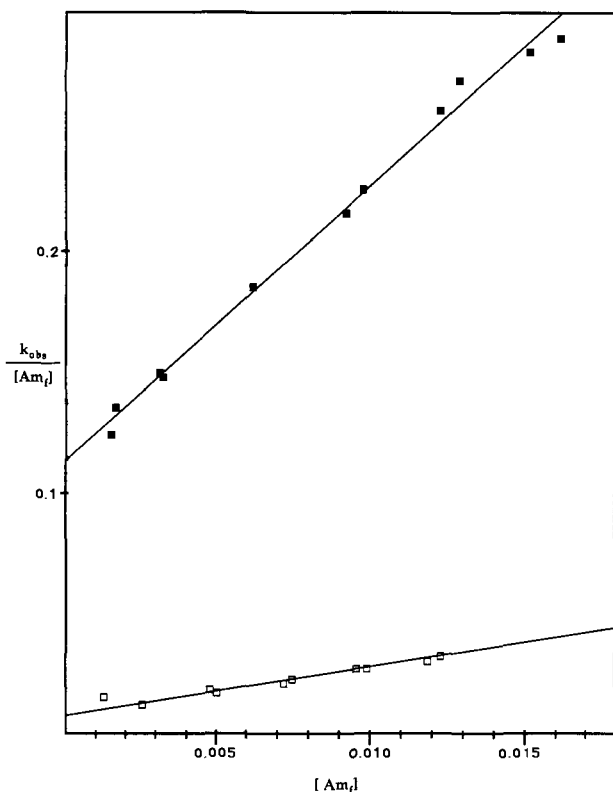


Figure 1. Plot of the pseudo-first-order rate constants divided by the concentration of benzylamine free base ($k_{\text{obs}}/[\text{Am}_f]$, $\text{s}^{-1} \text{M}^{-1}$) vs the concentration of benzylamine free base ($[\text{Am}_f]$, M), for the oxidation of benzylamine (■) and 1,1-dideuteriobenzylamine (□), by 9-decarboxymethoxatin at pH 8.81.

mole fraction of unhydrated quinone ($[Q_f]$), at any given pH, is provided by the composite form of eq 3. Equation 4 then becomes:

$$\frac{d[Q_f]}{dt} = (k_A[\text{Am}_f] + k_B[\text{Am}_f]^2)[Q_f] \left(\frac{a_H}{K_w K_1(1 + K_2) + a_H} \right) \quad (5)$$

with

$$k_{\text{obs}} = (k_A[\text{Am}_f] + k_B[\text{Am}_f]^2) \left(\frac{a_H}{K_w K_1(1 + K_2) + a_H} \right) \quad (6)$$

From eq 6, the slopes of plots of $k_{\text{obs}}/[\text{Am}_f]$ vs $[\text{Am}_f]$ equal $k_B(a_H/(K_w K_1(1 + K_2) + a_H))$ and the intercepts equal $k_A(a_H/(K_w K_1(1 + K_2) + a_H))$ (Figure 1). The pH dependent second-order and third-order rate constants for reaction of Q_f with Am_f are provided by k_A and k_B , respectively. These constants were determined from experiments at constant pH's with the known values of the term $a_H/(K_w K_1(1 + K_2) + a_H)$ at any given pH. The pH dependence of the log of k_A and the log of k_B is shown in Figure 2.

Concerning the two consecutive first-order reactions in the reaction of benzylamine with **1b** above pH 10, the more rapid reaction, as found with **1a**, is both first-order and second-order in Am_f (eq 4–6). The slower reaction showed only a first-order dependence on Am_f (eq 7). The pH-independent value of the second-order rate constant (k_C) for the reaction of Q_f with Am_f was

$$\frac{-d[Q_f]}{dt} = k_C[\text{Am}_f][Q_f] \left(\frac{a_H}{K_w K_1(1 + K_2) + a_H} \right) \quad (7)$$

determined as $(1.9 \pm 1) \times 10^{-2} \text{M}^{-1} \text{s}^{-1}$.

Kinetic deuterium isotope effects were determined at two pH values with PhCH_2NH_2 (0.015–0.15 M) and PhCD_2NH_2 (0.01–0.1 M) in parallel experiments. The kinetic deuterium isotope effects on k_A and k_B were determined from the ratio of

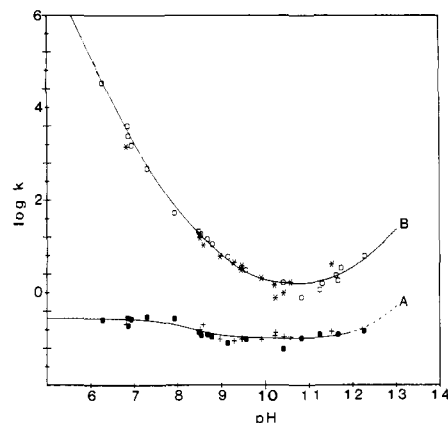


Figure 2. pH rate profiles for the oxidation of benzylamine by 9-decarboxymethoxatin and methoxatin at 25 °C. Plotted is the log of the rate constants for the reaction of unhydrated quinone species (Q_f) with benzylamine free base (Am_f). Plot A is of $\log k_A$ ($\text{s}^{-1} \text{M}^{-1}$) vs pH [(●) 9-decarboxymethoxatin (+) methoxatin] while plot B is of $\log k_B$ ($\text{s}^{-1} \text{M}^{-2}$) vs pH [(○) 9-decarboxymethoxatin; (*) methoxatin].

the slopes and intercepts of plots of $k_{\text{obs}}/[\text{Am}_f]$ vs $[\text{Am}_f]$ (Figure 1). The kinetic deuterium isotope effect on k_A varies from 14.3 at pH 8.81 to 3.6 at pH 11.69 whereas the isotope effect on k_B was determined as 5.7 at both pH 8.81 and 11.69.

Product analysis ($[Q_f] = 7.6 \times 10^{-5} \text{M}$ and $[\text{Am}_f] = 0.05 \text{M}$) was initiated by adjusting the acidity of the spent reaction solution to pH 4 with argon-purged 1.0 M HCl (O_2 -free N_2 atmosphere) prior to anaerobic HPLC analysis (the Experimental Section). The spectra and retention times of PhCHO, diols (**11a** and **11b**), aminophenols (**10a** and **10b**), and quinones (**1a** or **1b**) were identical to those of authentic samples. Characterization of **10a** was accomplished by the addition of a 20-fold excess of Am_f to a solution 3.02 mM in **1a** (pH 8.5) and, after 24 h at room temperature, separating the products by anaerobic thin-layer chromatography (the Experimental Section). The major product, a yellow band, was eluted with methanol. Anaerobic HPLC analysis showed that the spectrum and elution time of 16 min agreed with that of a product in solutions from kinetic runs. Aerobic oxidation of this compound regenerated **1a** and released ammonia. In multiple runs, the ratio of NH_3 (determined by a modification of the Nessler¹⁵ test) to **1a** (spectrophotometric) was 1 ± 0.25 . UV/vis spectra, obtained in the course of HPLC analysis, provided a $\lambda_{\text{max}} = 295 \text{nm}$ for **10a**. This value is in close agreement (300 nm for **10a** in CH_3CN) to that obtained by Itoh et al.^{11c} The λ_{max} of **10b** is at 289 nm.

When the spent kinetic solutions (starting with either **1a** or **1b**) were brought to a pH of ~ 4 and allowed to stand under an inert atmosphere, the ratio of aminophenol to diol was found to change with time. HPLC analysis showed that diol concentration increased while that of the aminophenol decreased. This indicates that some or all diol is derived from aminophenol. A pH of ~ 4 was employed in order to slow the rate of any air oxidation that might occur in the course of the HPLC analysis. This is a requirement even though the HPLC system was kept under an argon flush. The ratio of aminophenol (**10a** or **10b**) to diol (**11a** or **11b**) was determined from four duplicate HPLC analyses. The relative concentrations of aminophenol and diol were determined from the absorbance of the *normalized* spectra at their isosbestic point at the time of their elution (Table I and Figure 3). Due to the noted conversion of aminophenol to diol, the ratios aminophenol/diol of Table I must be considered as minimal.

HPLC analysis of the reaction mixtures indicated the presence of an unknown species with a retention time of 23 min for both **1a** and **1b**. With **1a**, the species could not always be detected due to its low concentration. Addition of reducing agents (NaBH_3CN or $\text{Na}_2\text{S}_2\text{O}_4$) to spent kinetic solutions, when using **1b** at pH 8.96, did not affect the spectrum of this product ($\lambda_{\text{max}} = 301, 338 \text{nm}$ from **1a**, $\lambda_{\text{max}} = 297, 332 \text{nm}$ from **1b**). This indicates that this species is fully reduced. Formation of this uncharacterized species could come about in the second of the two reactions monitored

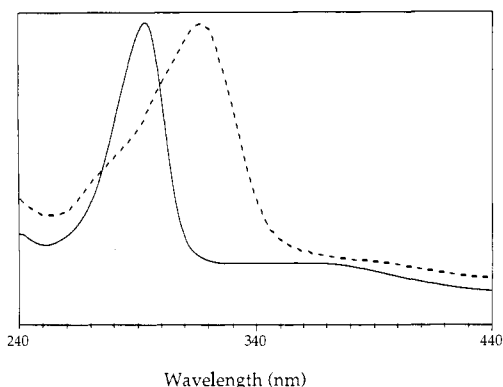


Figure 3. Normalized UV/vis spectra of diol **11a** (---) and aminophenol **10a** (—) at pH 3. The spectra were obtained from the HPLC product analysis of the reaction of methoxatin with benzylamine, using a diode array UV detector.

in the reactions of **1b** with Am_f at high pH.

Sleath et al. reported formation of oxazole derivatives when 7,9-didecarboxymethoxatin (**1c**) was used as an aerobic autorecycling catalyst in the oxidation of amines (eq 2).^{11b} After 24 h in the presence of air, **1b** was found to be converted to the oxazole **7b** at pH 8.96 in a solution containing initially **1b** (3.8×10^{-5} M) and Am_f (0.05 M). HPLC analysis showed a small amount of the species eluting at 23 min remaining. A reasonable assumption is that this compound is a precursor to the oxazole. After 24 h of the aerobic reaction of **1a** with benzylamine, most of **1a** remained; however, some oxazole **7a** was also detected. The assignment of the oxazole structures **7a,b** ($R = Ph$) is based upon a comparison of their characteristic spectra to that of the authentic **7c**.

Oxidation of aminophenol 10a (6.0×10^{-5} M) by methoxatin (1.52×10^{-5} M) was studied in buffered solutions between pH 6 and 12. The time course for appearance of diol **11a** was followed at 300 or 310 nm (Figure 4). Complete conversion to **11a** was confirmed by HPLC. As with most imines of ammonia, hydrolysis of Im is expected to be rapid, such that $[Q_i]$ remains constant throughout the reaction. The time course for spectral changes

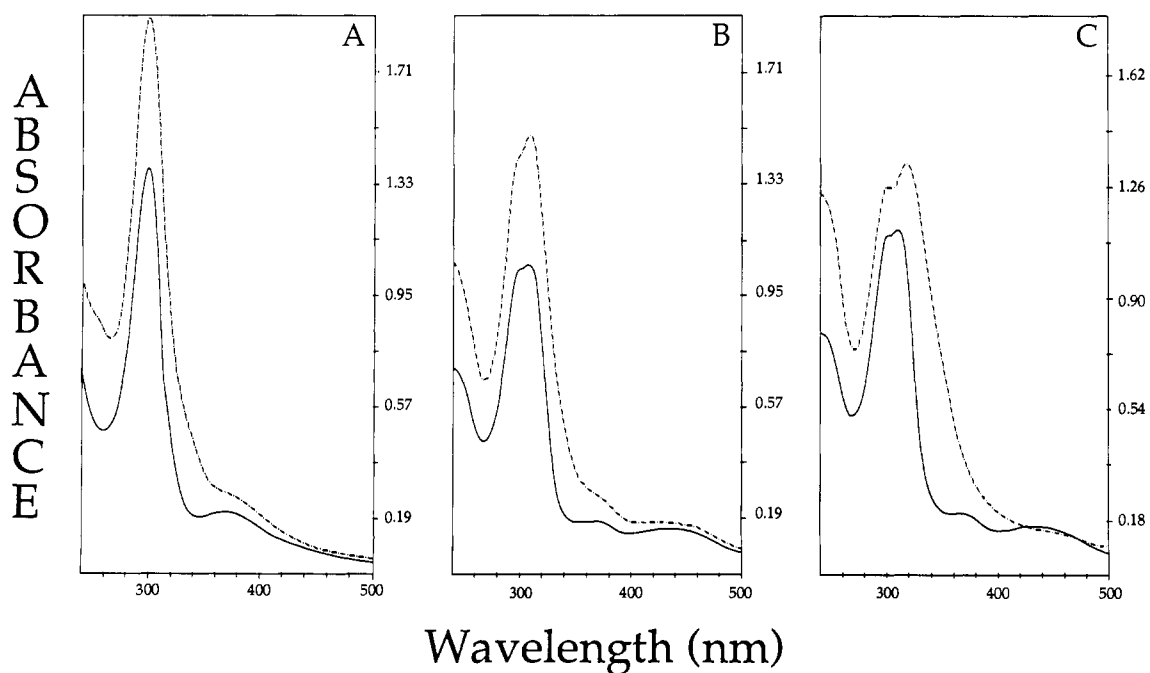


Figure 4. Initial (—) and final spectra (---) obtained from the oxidation of aminophenol **10a** (6.0×10^{-5} M, concentration obtained from the absorbance of a reoxidized solution of **10a**) by **1a** (1.5×10^{-5} M). The initial spectrum is that of aminophenol and the final spectrum is of the mixture of diol **11a** and **1a**: (A) pH 6.04 (phosphate buffer), the ϵ of aminophenol **10a** at 300 nm is $\sim 24\,000$ $M^{-1} cm^{-1}$; (B) pH 8.95 (borate buffer), the ϵ of aminophenol **10a** at 300 nm is $\sim 17\,700$ $M^{-1} cm^{-1}$; (C) pH 12.01 (HO^-/H_2O buffer), the ϵ of aminophenol **10a** at 310 nm is $\sim 15\,400$ $M^{-1} cm^{-1}$. (C) pH 12.01 (HO^-/H_2O buffer), the ϵ of aminophenol **10a** at 310 nm is $\sim 15\,400$ $M^{-1} cm^{-1}$.

Table I. Ratio of Aminophenol (AP = **10a** or **10b**) to Diol (**11a** or **11b**) in the Oxidation of Benzylamine by Methoxatin and 9-Decarboxymethoxatin^a

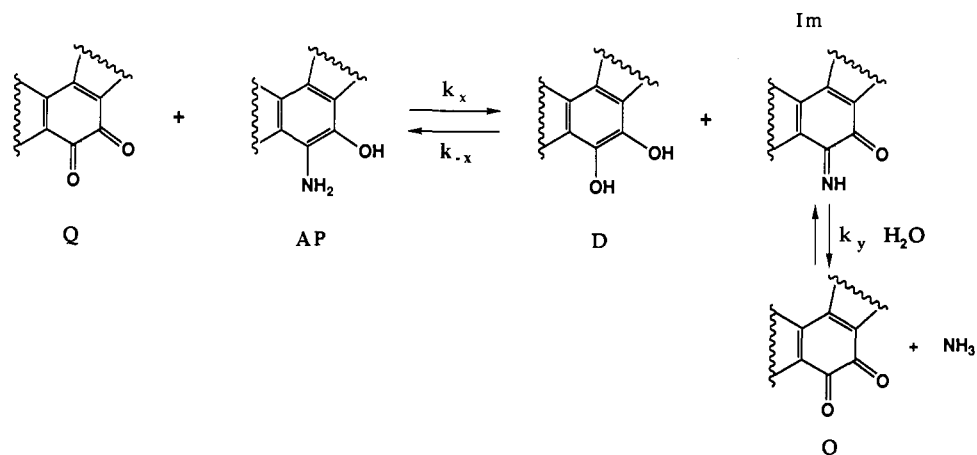
oxidant	pH	ratio AP/diol
methoxatin (1a)	8.77 ^{b,c}	10.5
methoxatin (1a)	10.75 ^c	1.1
methoxatin (1a)	11.85 ^c	0.9
9-decarboxymethoxatin (1b)	8.96 ^d	5.2
9-decarboxymethoxatin (1b)	10.75 ^d	1.1
9-decarboxymethoxatin (1b)	11.85 ^d	1.3

^a Conditions and instrumentation given in the Experimental Section. ^b Not acidified for the analysis. ^c Product ratio determined by measuring the absorbance at 300 nm. Retention times: aminophenol **10a** = 16 min; diol **11a** = 8.1 min; **1a** = 4.8 min; benzaldehyde = 11.6 min. ^d Product ratio determined by measuring the absorbance at 293 nm. Retention times: aminophenol **10b** = 16.6 min; diol **11b** = 6.1 min; **1b** = 5 min.

appears biphasic and may be computer-simulated to the sequence of reactions of Scheme I. A unique solution to the rate constants k_x , k_{-x} , and k_y could not be determined. Thus, at pH 6.78 (0.07 M phosphate buffer) equally good fits were obtained with $k_x = 165$ $M^{-1} s^{-1}$ and $k_{-x}/k_y = 400$, $k_x = 210$ $M^{-1} s^{-1}$ and $k_{-x}/k_y = 1600$, and $k_x = 325$ $M^{-1} s^{-1}$ and $k_{-x}/k_y = 7500$. A comparison of the $t_{1/2}$ values for the reaction of **1a** with Am_f and **1a** with **10a** shows that the latter is product-determining below pH 7.

An increase in buffer concentration (phosphate, borate, carbonate, or hydroxide) results in a decrease in the rate of diol formation. This cannot be explained other than by association of reactants with buffer so as to disfavor the electron-transfer reaction. At a constant μ (with KCl) the inclusion of increasing concentrations of phosphate buffer (0.04–0.1 M, pH 7) to a solution containing **1a** (3.8×10^{-5} M) results in an easily determined increase in absorbance of **1a** at 248, 269, and 330 nm indicative of an undetermined interaction of methoxatin and buffer. In the oxidation Am_f by **1a**, the autocatalytic reactions of Scheme I may explain the conversion of **10a** product to **11a** on acidification of spent kinetic solutions. Trace amounts of oxygen introduced with the acid solution could generate quinone, which triggers the autocatalytic reaction.

Scheme I



Scheme II

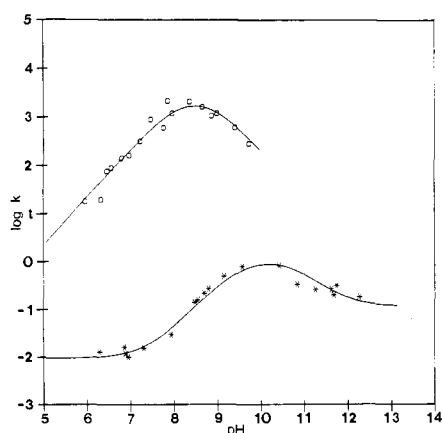
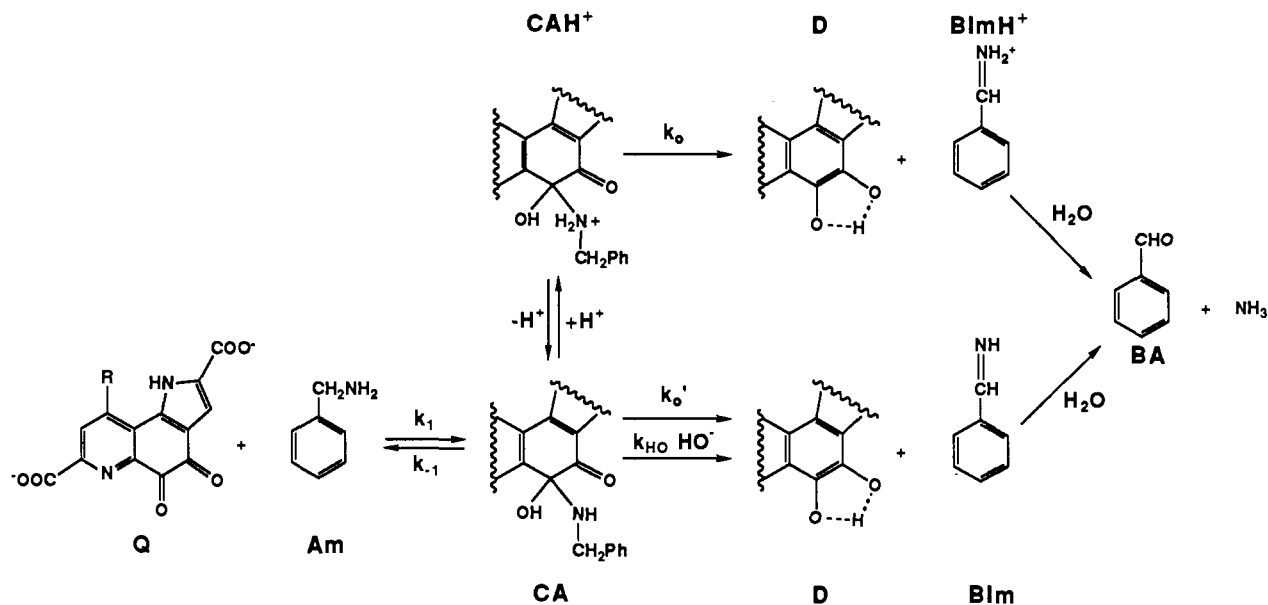


Figure 5. Comparison of the pH rate profiles for the oxidation of benzylamine by 9-decarboxymethoxatin (*) and by bovine plasma amine oxidase (O).⁷ In the case of 9-decarboxymethoxatin there is plotted the log of the apparent third-order rate constant for the benzylamine-catalyzed oxidation of benzylamine by the quinone. The pH-dependent rate constant (k_B' , $s^{-1} M^{-2}$) is calculated on the basis of the total concentration of benzylamine and its conjugate acid and the total concentration of quinone and its hydrate. For the enzymatic reaction the log of the pH-dependent constant k_{cat}/K_m ($s^{-1} M^{-1}$) has been plotted.

Discussion

Comparison of Benzylamine Oxidation by Quinone Catalyzed by Benzylamine and by Bovine Plasma Amine Oxidase

(BPAO). Figure 5 shows the pH rate profile for the oxidation of benzylamine by 9-decarboxymethoxatin (**1b**) when a second molecule of benzylamine acts as catalyst. Each point represents the log of the apparent third-order rate constant, k_B' (eq 8). In

$$\text{rate} = k_B' [9\text{-decarboxymethoxatin}] [Am_t]^2 \quad (8)$$

eq 8 total benzylamine is Am_t (and $[Am_t] = [Am_f] + [AmH^+]$). The pH dependence of k_{cat}/K_m for the oxidation of benzylamine by BPAO is also shown in the figure. These data were obtained by digitization of a plot presented by Farnum et al.⁷ The value of $(k_{cat}/K_m)/k_B'$ at maximum activities is equal to an effective molarity of $\sim 10^3$ M. Thus, the kinetic advantage of the enzymatic catalysis when compared to amine catalysis is in the minimal range of efficiency for enzymatic reactions.¹⁸ Values of k_B' for 9-decarboxymethoxatin (**1b**) and methoxatin (**1a**) are almost indistinguishable between pH 6 and 12 such that mechanistic details obtained from the experiments with one oxidant may be confidently extrapolated to the other.

Two kinetic pK_a values are obtained from the fitting of the "bell-shaped" portion of the pH rate profiles (Figure 5) for the oxidation of benzylamine by both BPAO⁷ and **1b**. In the case of BPAO these have been attributed to the dissociation constant of $PhCH_2NH_3^+$ (which binds in its protonated form) and to a residue at the active site, which must remain unprotonated. In the oxidation of benzylamine by **1b**, the two kinetic pK_a values relate, in a complex manner, to the acid dissociation of

(18) Bruice, T. C. In *The Enzymes*; Boyer, P. D., Ed.; Academic: New York, 1971; Vol. 3, p 217.

Table II. Values of the Kinetic Constants from Schemes II and IV for the Oxidation of Benzylamine by 9-Decarboxymethoxatin and Methoxatin^a

param	value	param	value
k_a^b	$2.3 \times 10^{-1} \text{ s}^{-1} \text{ M}^{-1}$	k_2^c	$3.00 \times 10^{-6} \text{ s}^{-1} \text{ M}^{-1}$
k_b^b	$4.8 \times 10^{-2} \text{ s}^{-1}$	k_3^c	$4.38 \times 10^{-5} \text{ s}^{-1} \text{ M}^{-1}$
k_c^b	$< 4.2 \text{ s}^{-1} \text{ M}^{-1}$	k_4^c	$1.27 \times 10^{-5} \text{ s}^{-1} \text{ M}^{-1}$
K_{app}^b	7.6×10^{-9}	k_5^c	$8.03 \times 10^{-3} \text{ s}^{-1} \text{ M}^{-1}$
K_1^c	$3.40 \times 10^4 \text{ M}^{-1}$	$K_{H_2O}^c$	1.79×10^{-3}
K_H^c	$2.15 \times 10^7 \text{ M}^{-1}$	K_{OH}^c	1.05 M^{-1}

^a Obtained by computer simulation of the kinetic data of Figure 2 using eq 9 (curve A) and eq 15–17 (curve B). ^b From eq 9. ^c From Scheme IV.

Chart I

$$k_a = k_1 \quad k_b = k_0'k_1/(k_{-1} + k_0')$$

$$k_c = k_{HO}k_1/(k_{-1} + k_0') \quad K_{app} = (k_{-1} + k_0')K_a/k_0$$

PhCH₂NH₃⁺ and an apparent pK_a (i.e., $K_wK_1(1 + K_2)$) of eq 3) for hydration of the quinone (eq 1a). Hydration of enzyme-bound **1a** has not been examined so that one cannot discard the hydration equilibria in interpreting the pH dependence of the enzymatic reaction.

Comparisons of the rate constants for the oxidation of PhCH₂NH₂ and PhCD₂NH₂ by BPAO between pH 5 and 10 has established¹⁹ that $(k_{cat}^H/K_m^H)/(k_{cat}^D/K_m^D)$ lies between 13 and 15. From eq 5, the reactions of **1a** and **1b** with Am_f are both first- and second-order in Am_f ($(k_A[Am_f] + k_B[Am_f]^2)/[Q_f]$, where Q_f is unhydrated **1a** or **1b**). For lyate species catalyzed oxidation of benzylamine by **1b** values of k_A^H/k_A^D are 14.3 (pH 8.81) and 3.6 (pH 11.69). In the benzylamine general-base-catalyzed oxidation of benzylamine by **1b** values of k_B^H/k_B^D are 5.7 at pH's 8.81 and 11.69. Clearly, proton abstraction is fully rate-limiting in the enzymatic reaction. For the oxidation of benzylamine by **1b** in solution, proton abstraction is at least partially rate-limiting in the lyate-catalyzed oxidation (k_A) and when benzylamine is both substrate and catalyst (k_B).

Mechanisms of the Lyate Species Catalysis of the Oxidation of Benzylamine. Curve A (Figure 2) was obtained by computer-fitting the experimental log k_A points to the empirical eq 9.

$$k_A = \frac{k_a a_H + k_b K_{app}}{K_{app} + a_H} + k_b + \frac{k_c K_w}{a_H} \quad (9)$$

The terms of eq 9 may be related to the reactions of Scheme II. An assumption of steady state in [CA] and [CAH⁺] provides eq 10. Below neutrality, eq 10 reduces to the form of the first term

$$\frac{-d[CA]}{dt} = \frac{k_1[Am_f][Q_f](k_0 a_H^2 + k_0'K_a a_H + k_{HO}K_a K_w)}{k_{-1}K_a a_H + k_0 a_H^2 + k_0'K_a a_H + k_{HO}K_w K_a} \quad (10)$$

of eq 9 (eq 11), which is consistent with H₂O catalysis (k_0 and

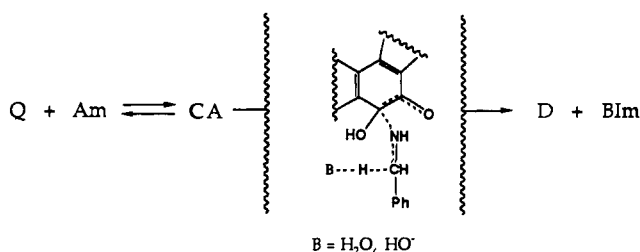
$$\frac{-d[CA]}{dt} = \left(\frac{k_1 a_H + k_0'K_a/k_0}{(k_{-1} + k_0')K_a/k_0 + a_H} \right) [Am_f][Q_f] \quad (11)$$

k_0') of the reaction of CA and CAH⁺ to provide D (Scheme III). Above neutrality, eq 10 reduces to eq 12. Assuming that the term

$$\frac{-d[CA]}{dt} = \left(\frac{k_0'k_1 + k_{HO}k_1K_w/a_H}{k_{-1} + k_0'} \right) [Am_f][Q_f] \quad (12)$$

$$1 + (k_{HO}K_w)/a_H(k_{-1} + k_0') \ll 1.0, \text{ eq 12 provides eq 13. The terms of } k_a \text{ and } K_{app} \text{ can be calculated from eq 11 while } k_b \text{ and } k_c \text{ may be determined with eq 13 (Table II). The relationship of } k_a, k_b,$$

$$\frac{-d[CA]}{dt} = \left(\frac{k_0'k_1 + k_{HO}k_1K_w/a_H}{k_{-1} + k_0'} \right) [Am_f][Q_f] \quad (13)$$

Scheme III**Chart II**

$$k_d = \frac{k_1 k_H k_3}{k_{-1} k_{-H} K_a} = \frac{K_1 K_H k_3}{K_a}$$

$$k_e = \frac{k_1 k_2}{k_{-1} K_a} + \frac{k_1 k_H k_5}{k_{-1} k_{-H}} = \frac{K_1 k_2}{K_a} + K_1 K_H k_5$$

$$k_f = \frac{k_1 k_4}{k_{-1}} + \frac{k_1 k_{H_2O} k_5}{k_{-1} k_{-H_2O}} = K_1 k_4 + K_1 K_{H_2O} k_5$$

$$k_g = \frac{k_1 k_{OH} k_5}{k_{-1} k_{-OH}} = K_1 K_{OH} k_5$$

k_c , and K_{app} to the constants k_0 , k_0' , k_{HO} , and K_a of eq 11 and 13 is shown in Chart I. The values of the kinetic constants obtained by computer-fitting of the experimental values of log k_A to eq 9 (line A of Figure 2) are included in Table II. The individual values of k_0 , k_0' , k_{HO} , and K_a cannot be determined because of the composite form of the constants k_b , k_c , and K_{app} .

Mechanism of Benzylamine Catalysis of the Oxidation of Benzylamine. The apparent third-order rate constant k_B pertains to benzylamine oxidations, which are second-order in amine. The pH dependence of k_B is correlated by curve B of Figure 2. The slope of curve B changes with increase in pH from -2 (second order in H⁺, pH < 7.5) to -1 (first order in H⁺, pH 7.5–9.5) to 0 (pH 9.5–11.5) to +1 (first order in HO⁻, above pH 11.5). The rate of product formation is described by eq 14

$$\frac{-d[\mathbf{1a} \text{ or } \mathbf{1b}]}{dt} = \left(k_d a_H^2 + k_e a_H + k_f + k_g \frac{K_w}{a_H} \right) [Am_f]^2 [Q_f] \quad (14a)$$

where

$$k_B = \left(k_d a_H^2 + k_e a_H + k_f + k_g \frac{K_w}{a_H} \right) \quad (14b)$$

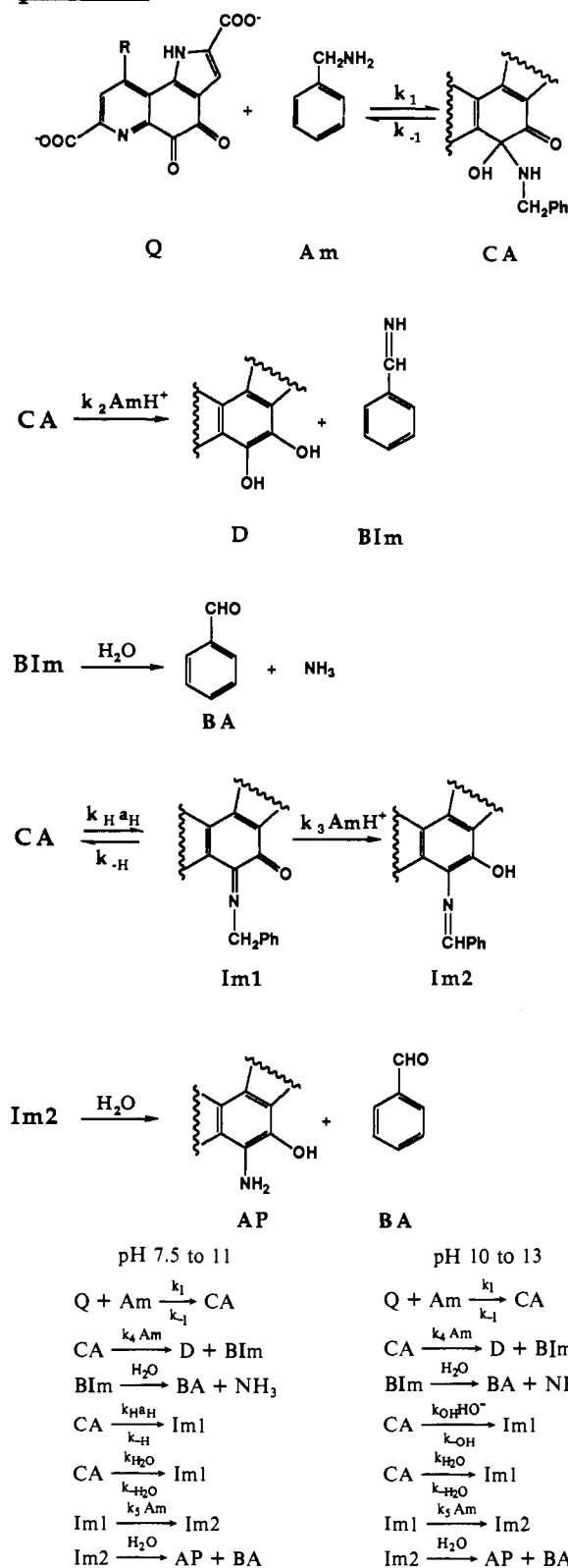
From product analysis (Table I), the working mechanism must allow for preferential formation of aminophenols (**10a** or **10b**) over diols (**11a** or **11b**) below pH 10 and the formation of aminophenols and diols in at least a 1:1 ratio above pH 10. The mechanisms of Scheme IV are consistent with the product analysis and the kinetic data. Common to each mechanism is the formation of a carbinolamine intermediate (CA). Abstraction of the benzylic α -proton of CA provides diol and BIm whereas dehydration of CA provides the imine Im1, which, after benzylic α -proton abstraction and hydrolysis, gives the products AP and BA. Assuming steady state in CA and Im1, the benzylamine-catalyzed formation of aminophenol (**10a** or **10b**) and diol (**11a** or **11b**) is described, dependent upon pH, by eq 15–17. By comparison of the empirical

$$\text{pH } < 7.5 \quad \frac{-d[Q]}{dt} = \left(\frac{k_1 k_H k_3 a_H^2}{k_{-1} k_{-H} K_a} + \frac{k_1 k_2 a_H}{k_{-1} K_a} \right) [Q_f][Am_f]^2 \quad (15)$$

$$\text{pH } 7.5\text{--}11 \quad \frac{-d[Q]}{dt} = \left(\frac{k_1 k_H k_3 a_H}{k_{-1} k_{-H}} + \frac{k_1 k_{H_2O} k_5}{k_{-1} k_{-H_2O}} + \frac{k_1 k_4}{k_{-1}} \right) [Q_f][Am_f]^2 \quad (16)$$

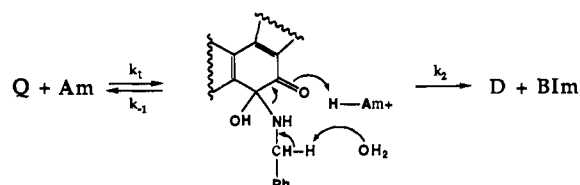
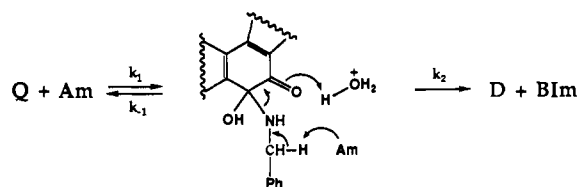
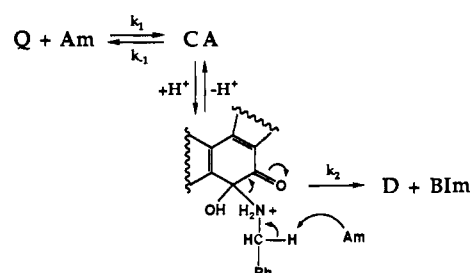
$$\text{pH } 10\text{--}13 \quad \frac{-d[Q]}{dt} = \left(\frac{k_1 k_{OH} k_5 K_w}{k_{-1} k_{-OH} a_H} + \frac{k_1 k_{H_2O} k_5}{k_{-1} k_{-H_2O}} + \frac{k_1 k_4}{k_{-1}} \right) [Q_f][Am_f]^2 \quad (17)$$

Scheme IV

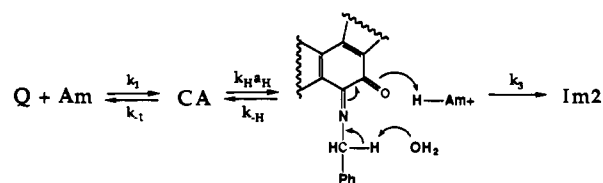
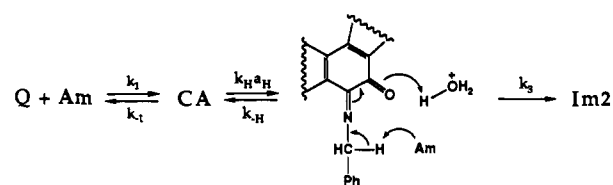
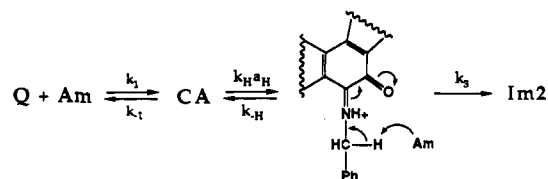
pH < 7.5

eq 14 to eq 15–17, the constants k_d , k_e , k_f , and k_g are defined as in Chart II. The numerical values of the constants k_d , k_e , k_f , and k_g were obtained by iteration in the computer-fitting of the data of curve B, Figure 2, by use of eq 14b. From the equalities of Chart II, there was calculated the numerical values of k_1/k_{-1} (K_1), k_H/k_{-H} (K_H), k_{H_2O}/k_{-H_2O} (K_{H_2O}), k_{OH}/k_{-OH} (K_{OH}), k_2 , k_3 , k_4 , and k_5 (Table II). The value of the constant K_1 was chosen such that log k_B points could be fit across the entire pH range. Knowing

Scheme V

a. Proton removal by H_2O , AmH^+ catalyzed.b. Proton removal by Am_f , H_3O^+ catalyzed.c. Proton removal from CAH^+ by Am_f .

Scheme VI

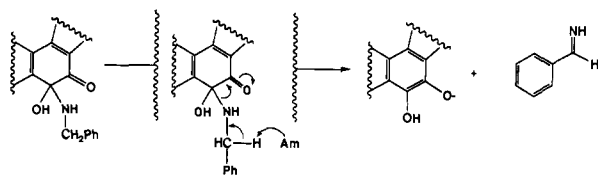
a. Proton removal by H_2O , catalyzed by AmH^+ .b. Proton removal by Am_f , catalyzed by H_3O^+ .c. Proton removal by Am_f on $Im1H^+$.

the values of K_a , K_1 , and k_d ($=K_1K_Hk_3/K_a$) provides the value of k_3K_H . The values of k_e ($=K_1K_Hk_5 + K_1k_2/K_a$) and k_f ($=K_1k_4 + K_1K_{H_2O}k_5$) are known, and the constants k_2 , k_4 , k_5 , and K_{H_2O} were chosen so that the ratio of the terms $[K_1K_Hk_3a_H^2/K_a + K_1K_Hk_5a_H + K_1K_{H_2O}k_5 + K_1K_{OH}k_5K_w/a_H]/[K_1k_2a_H/K_a + K_1k_4]$ (Chart II) is in close agreement to the product ratio amino-phenol/diol with changes in pH (Table I). The numerical value for K_{OH} was taken from the known value of k_g ($=K_1K_{OH}k_5$).

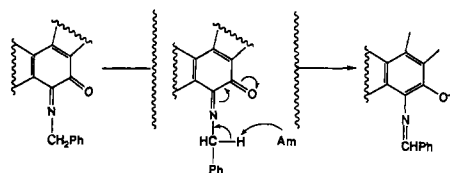
Below pH 7.5, conversion of CA to diol involves $PhCH_2NH_2$, H_3O^+ , or $PhCH_2NH_3^+$ or their kinetic equivalents as catalysts.

Scheme VII

to diol:



to aminophenol:



The competency of the three kinetically equivalent mechanisms of Scheme V may be tested by use of the values of the constants of Table II. The rate of CA disappearance for mechanism a in Scheme V is as shown in eq 18. In this mechanism H₂O serves

$$\frac{-d[\text{CA}]}{dt} = 3.00 \times 10^{-6} [\text{AmH}^+][\text{CA}] \quad (18)$$

as a general base for benzylic α -proton dissociation while AmH⁺ acts as a general acid to protonate the carbonyl oxygen in the course of its conversion to phenolate oxygen. This mechanism may be criticized on the basis that the weakest base is performing the role of general-base catalyst and, also, that phenolate and amine are of comparable basicity. In addition, general-acid protonation of insipient phenolate in the transition state should

not assist the reaction since the pK_a of the phenol species is not greatly removed from the kinetic experiments. From these considerations mechanism a of Scheme V may be discarded. Equation 18 may be rearranged to the kinetic equivalent expression of eq 19 (where $K_{\text{AmH}^+} = [\text{Am}][\text{H}_3\text{O}^+]/[\text{AmH}^+]$ and $K_{\text{aH}} =$

$$\begin{aligned} \frac{-d[\text{CA}]}{dt} &= \frac{k_2}{K_{\text{AmH}^+}} [\text{Am}][\text{H}^+][\text{CA}] \\ &= \frac{k_2 K_{\text{aH}}}{K_{\text{AmH}^+}} [\text{Am}][\text{H}_3\text{O}^+][\text{CA}] \\ &= 6.1 \times 10^5 [\text{H}_3\text{O}^+][\text{Am}][\text{CA}] \quad (19) \end{aligned}$$

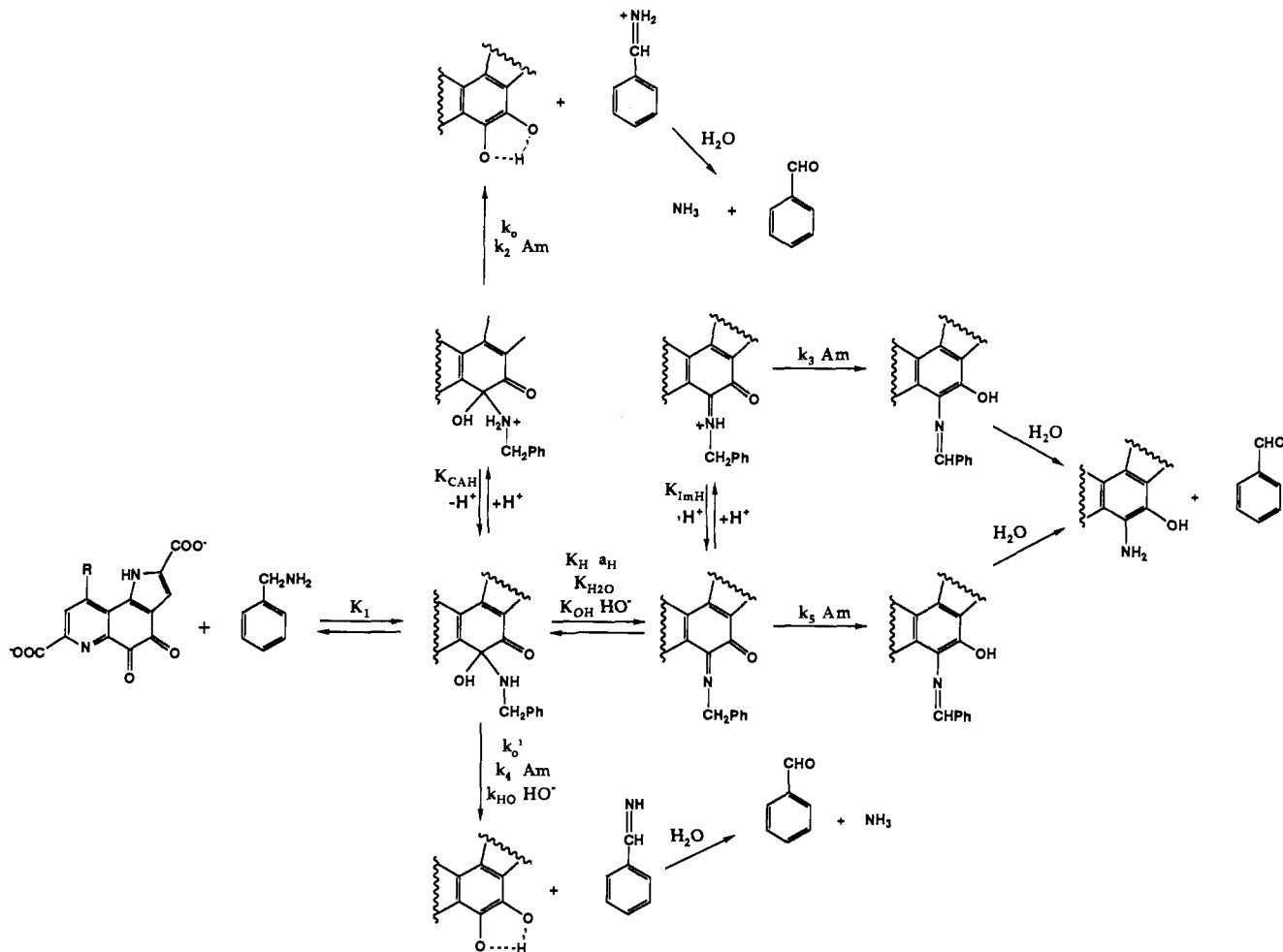
[H₂O][H⁺]/[H₃O⁺]). Equation 18 can (as eq 19) also be expressed as a kinetic equivalent as shown in eq 20. The rate

$$\begin{aligned} \frac{-d[\text{CA}]}{dt} &= \frac{k_2 K_{\text{aH}} K_{\text{CAH}}}{K_{\text{AmH}^+}} [\text{Am}][\text{CAH}^+] \\ &= 6.1 \times 10^5 K_{\text{CAH}} [\text{Am}][\text{CAH}^+] \quad (20) \end{aligned}$$

constant of eq 19 is below diffusion control, and the mechanism is kinetically plausible. Since the ionization constant for CAH⁺ (K_{CAH}) is certainly <1, the mechanism of eq 20 is also kinetically plausible. From eq 19 and 20 one can construct the mechanisms of b and c (Scheme V), respectively. Mechanism c must be preferred over b. In b the general-acid catalysis of oxygen protonation by H₃O⁺ would be of little importance due to the moderate pK_a of the phenol substituent in the product while placing the proton on the CA nitrogen in the starting state (as in mechanism c) should greatly increase the acidity of the benzylic α -proton undergoing general-base-catalyzed proton abstraction by Am_f.

Similar considerations may be offered concerning the mechanisms for the formation of aminophenols 10a and 10b below pH

Scheme VIII



7.5 (Scheme VI). The rate of conversion of Im1 to Im2 (mechanism a, Scheme VI) may be described by eq 21. Rear-

$$\begin{aligned} \frac{-d[\text{Im}1\text{H}^+]}{dt} &= k_3[\text{Im}1][\text{AmH}^+] \\ &= 4.38 \times 10^{-5}[\text{Im}1][\text{AmH}^+] \quad (21) \end{aligned}$$

rangement of eq 21 provides the rate expression for the formation of Im2 through mechanism b of Scheme VI (eq 22). Mechanism

$$\begin{aligned} \frac{-d[\text{Im}1\text{H}^+]}{dt} &= \frac{k_3 K_{\text{aH}}}{K_{\text{AmH}^+}} [\text{Im}1][\text{Am}][\text{H}_3\text{O}^+] \\ &= 8.95 \times 10^6 [\text{Im}1][\text{Am}][\text{H}_3\text{O}^+] \quad (22) \end{aligned}$$

b is associated with a rate constant less than diffusion control and, therefore, kinetically competent. Equation 23 is the kinetic equivalent of eq 21 and is an expression in accord with mechanism c. Although the value of K_{ImH^+} is unknown, it is expected to be

$$\begin{aligned} \frac{-d[\text{Im}1\text{H}^+]}{dt} &= \frac{k_3 K_{\text{aH}} K_{\text{ImH}^+}}{K_{\text{AmH}^+}} [\text{Im}1\text{H}^+][\text{Am}] \\ &= 8.95 \times 10^6 K_{\text{ImH}^+} [\text{Im}1\text{H}^+][\text{Am}] \quad (23) \end{aligned}$$

near 1×10^{-5} M such that the rate constant for formation of Im2 through mechanism c (Scheme VI) is below diffusion control. As in the dissociation of Scheme V, mechanism c is preferred. Above pH 7.5 general-base-catalyzed benzylic α -proton removal from CA or from Im1 is observed (Scheme VII).

Conclusions

Although 9-decarboxymethoxatin (**1b**) does not reconstitute activity to apo-D-glucose dehydrogenase from *A. calcoaceticus*,^{8b} the present study shows that its reactivity toward benzylamine in water is almost indistinguishable from that of methoxatin (**1a**). Also, the hydration equilibria and its pH dependence are almost the same for **1a** and **1b**. The finding that the 9-carboxyl group does not enhance quinoquinone electrophilicity supports the

suggestion that its essential role is in cofactor binding to apoenzyme. The rate of oxidation of benzylamine by **1a** or **1b**, as well as the ratio of diol/aminophenol (D/AP) products, is pH-dependent. The reaction of benzylamine with **1a** and **1b** involves the preequilibrium formation of benzylamine-quinone carbinol-amine intermediates (CA + CAH⁺). CA and CAH⁺ proceed to products by way of two general paths: (i) benzylamine, H₂O, or HO⁻ general-base α -benzylic proton abstraction and elimination to yield diol (**11a** and **11b**) plus the ammonia imine of benzaldehyde (BIm) and (ii) H₃O⁺, H₂O, or HO⁻-catalyzed dehydration providing imine species of quinone and benzylamine (Im1 and Im1H⁺), which then undergo benzylamine general-base-catalyzed α -benzylic proton abstraction and elimination to provide the aminophenol imine of benzaldehyde (Im2). Hydrolysis of Im2 provides aminophenol (**10a** and **10b**) plus benzaldehyde. The reactions are summarized in Scheme VIII, and associated rate constants may be found in Table II. For both **1a** and **1b**, the aminotransferase mechanism yielding aminophenol is preferred below pH 10 (90% with **1a** and 80% with **1b** at ca. pH 9). It has been reported that amine oxidases react solely through this mechanism at pH < 9.^{12,13} We show that the low yields of aminophenol obtained in previous product studies^{11b,c} are attributable to the autocatalytic oxidation of aminophenol by quinone (as shown in Scheme I). The amine transferase reaction is mechanistically akin to the transamination reaction of pyridoxal with amino acids. The latter reaction was shown at an early date to be general-base-catalyzed.²⁰

Acknowledgment. This work was supported by a grant from the National Institutes of Health. E.J.R. is thankful to the University of California for support from the Chancellor's Graduate Research Associateship.

(20) (a) Auld, D. S.; Bruice, T. C. *J. Am. Chem. Soc.* **1967**, *89*, 2083, 2091, 2098. (b) Bruice, T. C.; Topping, R. M. *J. Am. Chem. Soc.* **1962**, *84*, 2448. (c) Bruice, T. C.; Topping, R. M. *J. Am. Chem. Soc.* **1963**, *85*, 1480, 1488.